OVERVIEW OF BEAM INSTRUMENTATION AND TUNING AT RIKEN RI BEAM FACTORY

N. Fukunishi*, M. Fujimaki, M. Kase, M. Komiyama, J. Ohnishi, H. Okuno, N. Sakamoto, H. Watanabe, T. Watanabe, K. Yamada, O. Kamigaito, RIKEN Nishina Center for Accelerator-Based Science, 2-1 Hirosawa, Wako, Saitama 351-0198, Japan
R. Koyama, SHI Accelerator Service Ltd., 1-17-6 Ohsaki, Shinagawa, Tokyo 141-0032, Japan

Abstract

The RIKEN Radioactive Isotope Beam Factory (RIBF) has been successfully producing the world's most intense medium-energy heavy-ion beams, such as 0.42-pμA-^{48}Ca and 24-pnA-^{124}Xe beams. Several types of beam monitor have played a vital role in attaining current performance levels, though many are of conventional design. This article gives an overview of RIBF beam instrumentation and introduces beam-tuning methods adopted by RIBF.

RI BEAM FACTORY

The Radioactive Isotope Beam Factory (RIBF) [1,2] started operation at the end of 2006 as the first second-generation radioactive beam facility. The RIBF experimentally investigates unknown areas of the nuclear chart, especially candidate nuclei essential to nucleosynthesis, by producing the world's most intense RI beams. For this purpose, beam intensities of 1 pμA are required for all stable ions, from hydrogen to uranium.

Table 1: Beam Intensities Obtained by RIBF

Ion	Energy (A MeV)	Beam Intensity	Acceleration Mode
^{4}He	320	1 pμA	Variable energy
^{18}O	290	0.45 pμA	AVF injection
^{18}O	345	1 pμA	Variable energy
^{48}Ca	345	0.42 pμA	Variable energy
^{124}Xe	345	24 pnA	Fixed energy
^{238}U	345	3.6 pnA	Fixed energy

The RIBF accelerator complex consists of two injector linac complexes (RILAC [3] and RILAC2 [4]), an injector AVF cyclotron [5] and four ring cyclotrons (RRC [6], fRC [7], IRC [8], and SRC [9]), including the world's first superconducting ring cyclotron SRC. Three acceleration modes are available in RIBF. The first is AVF injection mode, which is suitable for accelerating very light ions such as ^{4}He and ^{18}O. Here, AVF, RRC, and SRC are used in series. For medium-heavy elements such as ^{48}Ca and ^{70}Zn, a variable energy mode using RILAC, RRC, IRC, and SRC is employed. The third mode is a fixed energy mode where the new injector RILAC2 is utilized with all four ring cyclotrons, producing high intensity, very heavy ion beams such as ^{124}Xe and ^{238}U. Table 1 summarizes recent beam intensities. We have already extracted 1-pμA beams from SRC for light ions, and are steadily approaching 1 pμA for ^{48}Ca. The new RILAC2 injector was recently commissioned, and various RIBF upgrade programs are in progress to improve ^{124}Xe and ^{238}U beam intensities.

RIBF BEAM INTENSITY RANGE AND BEAM INSTUMENTATION

The typical beam intensity from SRC, the final-stage RIBF accelerator, is several microamperes. This corresponds to several tens of microamperes in the injector and intermediate-stage accelerators, because RIBF employs two-step charge-stripping schemes [10]. RIBF beam monitors also measure beams with intensities of 100 nA or less, because we begin beam tuning with an intensity-attenuated beam to avoid unnecessary hardware damage caused by poor accelerator optimization. The maximum beam power already obtained is 6.9 kW for a 345-MeV/nucleon-^{48}Ca beam, which requires careful beam tuning.

RIBF beam monitors are required to cover a wide beam-intensity region ranging from a few tens of nanoamperes to 100 μA. RIBF mainly uses conventional destructive beam monitors because they are suited to low-intensity beam operations. RIBF beam monitors are divided into two groups: monitors specific to cyclotrons, which include phase probes and radial probes, and monitors installed in beam lines and the two linac compexes, such as Faraday cups and beam profile monitors.

PROBES USED IN CYCLOTRONS

A typical cyclotron beam tuning procedure is as follows. Ions are injected into the cyclotron through a bending magnet, magnetic channels, and an electrostatic channel. Baffle slits at channel entrances detect beam loss, allowing best-fit determination of an ion injection orbit. Ions are accelerated if proper phases of accelerating RF fields are chosen under reasonable starting values for the cyclotron's isochronous magnetic fields. Step by step, ions are accelerated to higher energies by adjusting magnetic and RF fields. A radial probe plays an essential role in this procedure. The ions at last reach the cyclotron design energy, but the isochronous magnetic fields are still imperfect and are significantly improved by using a phase probe. After magnetic field tuning, RF phases are optimized with the use of the radial probe. Finally, ions are extracted from the cyclotron through an electrostatic

*fukunisi@ribf.riken.jp

ISBN 978-3-95450-119-9

channel, magnetic channels, and extraction bending magnets.

Phase Probe

A large cyclotron requires isochronous magnetic fields with better than 5 ppm accuracy, because total RF phases experienced by ions during acceleration are nearly 1 million degrees. Such accuracy can only be realized by iterated updates of the magnetic fields, based on precise measurements of beam phase using a "phase probe." A phase probe is a set of electrostatic pickup probes installed adjacently from the inner to outer radius, covering almost the entire acceleration region of the cyclotron. Table 2 summarizes values related to the pickup electrodes installed in RIBF cyclotrons.

Table 2: Phase-Probe Related Quantities

	RRC	fRC	IRC	SRC
Inner Radius (cm)	89	156	277	356
Outer Radius (cm)	356	330	415	536
Harmonics	9	12	7	6
Number of Pickup Electrodes	20	14	15	20
Typical Turn Numbers	300	180	180	340
RF Phase Advance (10^6 degrees)	0.97	0.78	0.45	0.73
Maximum RF Voltage (kV)	270	450	600	600
Signal Analysis	Osc.	LIA	LIA	LIA

Signals induced by ions passing through the phase probes are pre-amplified (20 dB) and analyzed by a digital oscilloscope (RRC) or lock-in amplifiers (LIA, SR844 [11]). Within fundamental and higher harmonic beam components, the harmonic giving the best signal-to-noise ratio is chosen in LIA analysis [12].

Figure 1(a) shows an example of an optimization procedure making isochronous magnetic fields of fRC. Magnetic field updates are performed as follows. We made numerical simulations and prepared a database of time shifts induced on all the pickup electrodes by given current changes in the cyclotron's main or trim coils (Fig. 1(b)). Using the database, new coil currents are determined by a least-square fitting method to minimize the RMS deviation of time shifts. The present method is not only valid for the cases where the first-order perturbation works well, but also effective for magnetic fields deviating sizably from an ideal isochronous magnetic field. In the latter case, it is sufficient that we introduce a reduction factor of 0.7 or so when applying the results of first-order calculations to an actual magnetic-field update. Several updates are required until isochronous magnetic fields with an RMS deviation of 0.1 ns are obtained. This

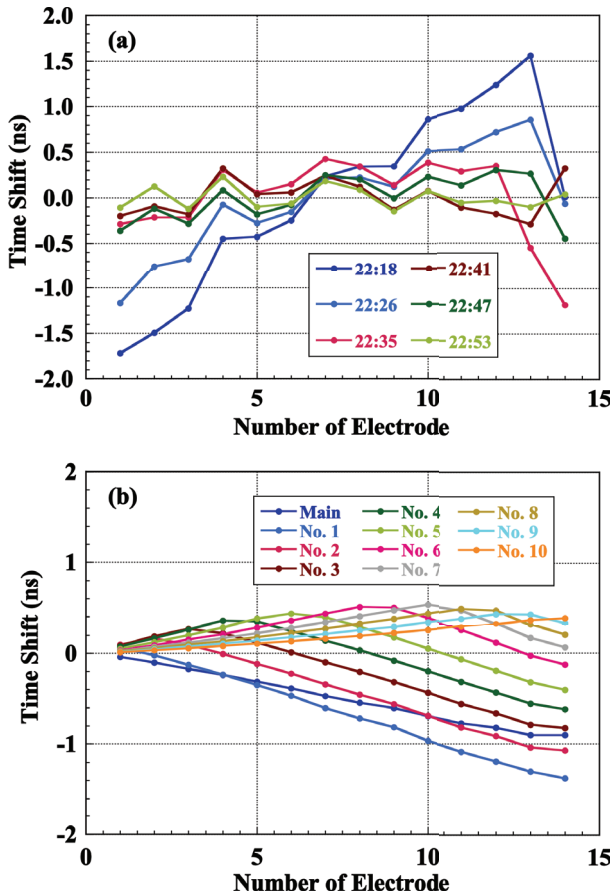

Figure 1: (a) Fitting procedure for fRC isochronous magnetic fields. Lines show the time of data acquisition. (b) Estimated time shifts caused by given current changes (0.03 A for the main coil and 3 A for trim coils) for fRC.

corresponds to a few RF degrees, and never degrades beam quality. This fitting procedure requires 1–2 h, depending on initial conditions.

Radial Probe

Our radial probes can measure beam intensities at any acceleration stage, that is, at any radial position in the cyclotrons, simultaneously giving turn patterns of accelerated ions. Integral and differential electrodes are mounted on the front end of a stainless-steel shaft (Fig. 2). These electrodes are inserted into a vacuum chamber of the cyclotron and are driven by a pulse motor from inner to outer, or vice versa.

An integral electrode measures beam intensity and performs initial adjustment of isochronous magnetic fields, as described previously. The integral electrodes used in RIBF are made of tantalum and cooled by water. Each electrode is designed to be sufficiently thick to stop completely accelerated ions, except for very light ions having a comparatively long range. For accurate beam-intensity measurements, it is better to avoid escape of secondary electrons produced by heavy-ion bombardments from the probe. If a magnetic field with sufficient strength acts on the probe, secondary electrons cannot escape the elec-

ISBN 978-3-95450-119-9

trode, and are finally absorbed by the top or bottom plate. Hence magnetic-field strength at the probe is important. Figure 3 summarizes magnetic field distributions along probe-moving lines for all the RIBF ring cyclotrons. Our operating experiences indicate that integral electrodes installed in RRC and IRC do not overestimate measured beam intensity in their outer radius region, suggesting that suppression of secondary electrons is sufficient for these two cyclotrons. On the contrary, enhancement by a factor of two or more is observed for fRC and SRC, caused by magnetic fields decreasing in their outer radius regions. Insufficient suppression of secondary electrons is a result of limited space available for the radial probes in fRC and SRC.

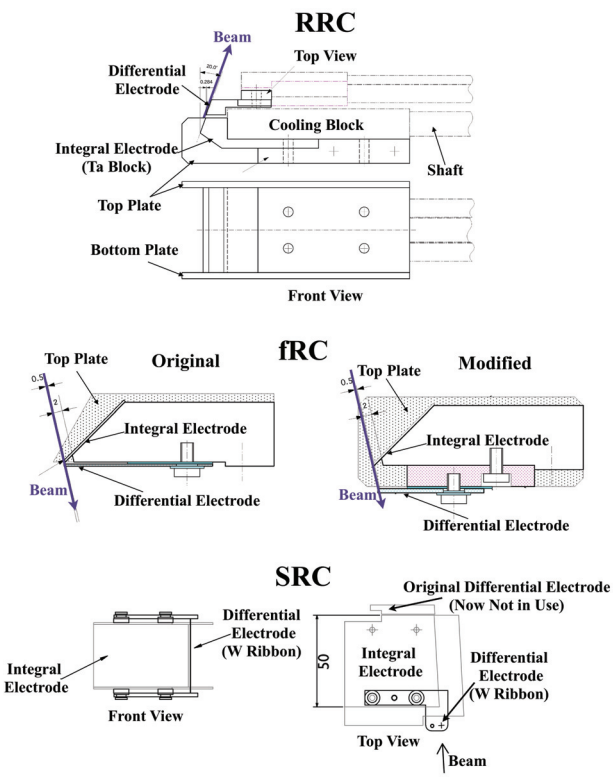

Figure 2: Radial probe designs of RRC, fRC, and SRC.

A differential electrode measures the turn pattern of accelerated ions. The turn pattern, the radial dependence of the beam density distribution, is directly related to beam quality, and hence reveals any existence of poor beam behavior. Secondary electrons are a potential problem for differential electrodes, as with integral probes. If secondary electrons emitted from an integral electrode sidewall hit the differential probe, it is impossible to obtain a realistic turn pattern because the secondary electrons may dominate the ion contribution of interest. Hence, the angle of the integral probe sidewall relative to the ion orbit and the position of the differential electrode relative to the integral electrode must be carefully designed. Conventional design is adopted for RRC and IRC, in which the angle of the tantalum block sidewall is parallel to the ion orbit and the differential electrode is placed just behind the integral electrode. This design works well for these two cyclotrons due to the existence of sufficient magnetic fields. We attempted to use the same design for fRC and SRC, but were unsuccessful. We have hence modified the design for fRC and SRC (Fig. 2). The modified design works well for SRC by placing the differential electrode before the integral electrode. In the case of fRC, the modified design allows us to obtain essential information on beam quality, but is still insufficient in that we find a decrease in zero current level of the turn pattern in the outer radius region (Fig. 4). This is further evidence of insufficient suppression of secondary electrons.

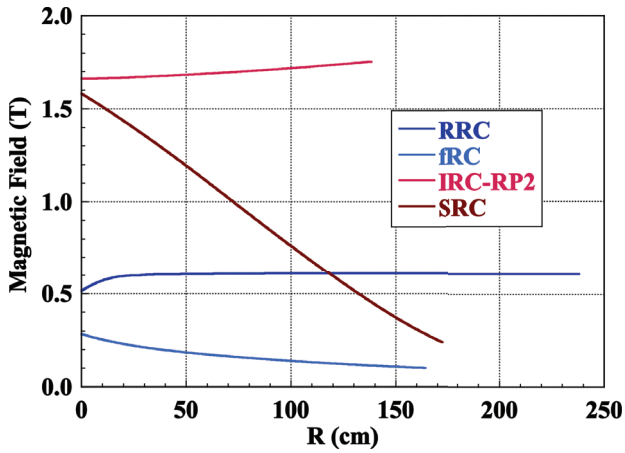

Figure 3: Magnetic fields calculated for the lines on which radial probes move. All the results are for ^{238}U acceleration. The "R = 0 cm" point corresponds to the injection radius for each cyclotron.

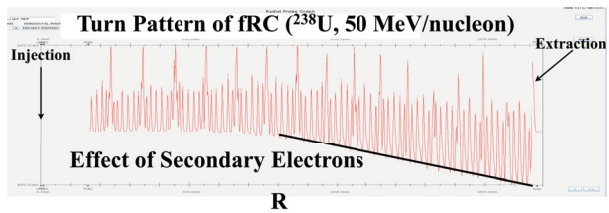

Figure 4: Effect of secondary electrons on fRC turn pattern.

Among the most important roles of the differential electrode is selecting the optimal RF field phases. Ions are accelerated at the top phases of accelerating RF fields to avoid unnecessary energy spread. In addition, a flat-topping cavity is introduced in fRC, IRC, and SRC to further reduce energy spread, and its phase must be closely matched. Figure 5 illustrates the sensitivity of beam quality according to FT phase settings. The RF phase optimization procedure is one of the most time-consuming beam tuning processes, owing to limited moving speeds of the differential electrodes.

One recent problem was serious damage to RRC's radial probe, caused by high-power beams, nearly breaking the integral electrode (Fig. 6). As mentioned previously, beam tuning begins with an intensity-attenuated beam, and then beam intensity is increased step by step to its maximum. In this process, the space charge effect and

ISBN 978-3-95450-119-9

beam loading effect are expected to change the optimal RF phases. We therefore frequently measure turn patterns with relatively high-intensity beams. Because the existing radial probes do not have an protection system with the high-power beams, we failed to avoid serious damage to the radial probe. Increased cooling capacity or the introduction of an interlock system is required.

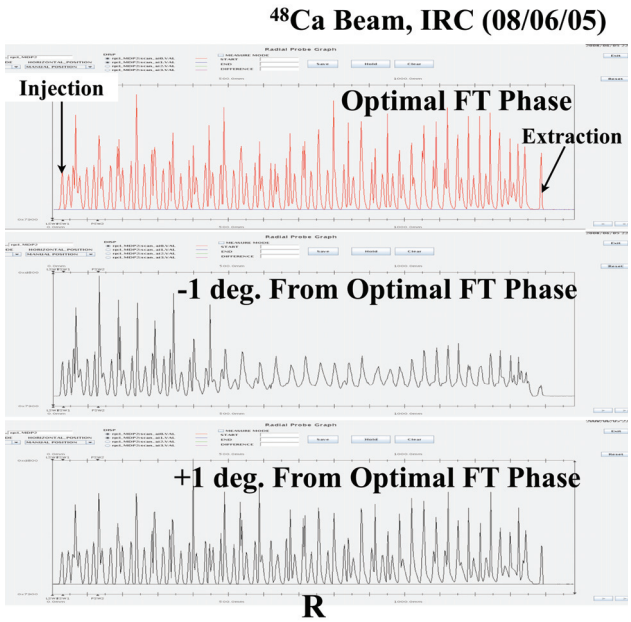

Figure 5: Comparison of IRC turn patterns with different parameters of FT phase in the case of a 114-MeV/nucleon-^{48}Ca beam.

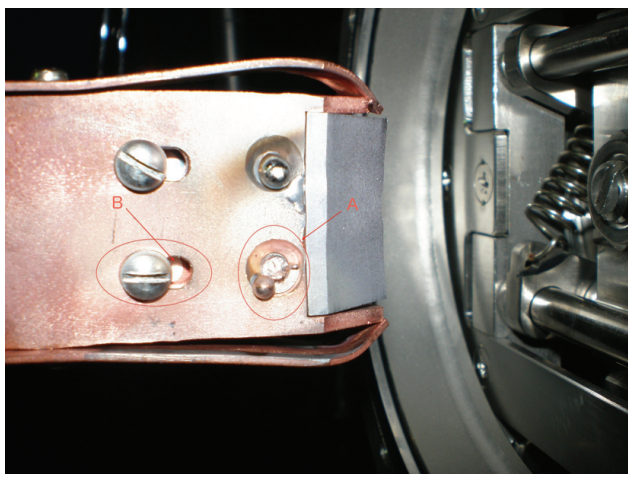

Figure 6: Damaged RRC radial probe. High-power beams melted two bolts used to fix the integral electrode to its cooling plate. The resulting heat deformed the top and bottom plates attached to the integral electrode.

BEAM LINE MONITORS

Table 3 summarizes the beam monitors used in the RIBF beam transport lines with the length of the beam lines. Some lines partly overlap, so the total number of monitors installed for all RIBF beam lines is less than the sum of the numbers listed in Table 3.

Wire scanner beam profile monitors (PF) are commonly used to measure beam position and profile. Three measuring wires are mounted in the horizontal and vertical directions, and a middle line between them for information redundancy. PFs are used for beam centering and emittance analysis, as usual [2]. PFs cover the beam-intensity region ranging from 0.1 nA to 1 μA using 4-channel amplifiers.

Table 3: Summary of Beam Line Monitors

	L (m)	PF	FC	PS	PP
RILAC–RRC	71	19	10	5	4
RILAC2–RRC	39	11	6	3	2
AVF–RRC	39	12	6	3	3
RRC–fRC	81	18	11	3	3
RRC–IRC	89	20	10	3	4
fRC–IRC	120	25	10	3	4
RRC–SRC	137	28	12	3	4
IRC–SRC	54	11	5	2	2

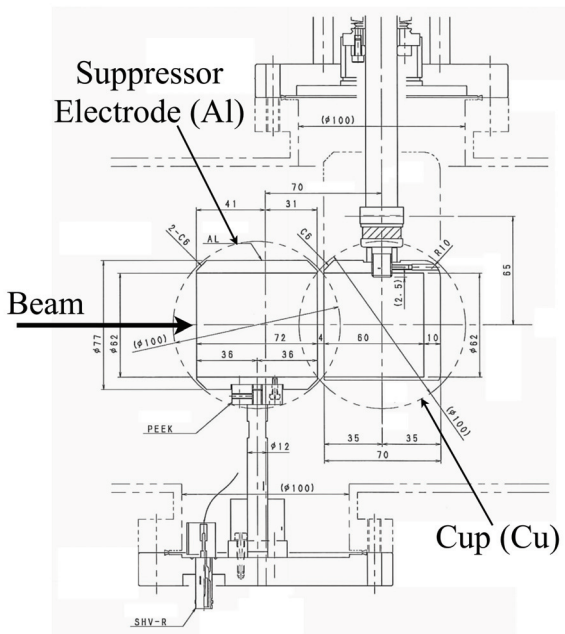

Figure 7: Standard Faraday cup design.

Faraday cups (FC) stop beams, allowing for not only beam intensity measurements, but also section-by-section tuning. FCs are capable of measuring a beam current ranging from 1 nA to 100 μA. Figure 7 illustrates the standard design, in which a shallow cup is adopted due to the importance of compactness. A compact cup is easily inserted into or removed from a beam path, but the price of compactness is again increased difficulty in completely suppressing secondary electrons. To mitigate overestima-

ISBN 978-3-95450-119-9

tion caused by insufficient suppression of secondary electrons, a long electron suppressor producing a nearly uniform suppression field was introduced, instead of conventional ring-type suppressors. However, there remains a 10–20% overestimation, which is strongly indicated by comparing measured beam intensities with those measured by the radial probes of RRC and IRC. In addition, FCs are a major source of residual radiation in the beam lines, so nondestructive beam current monitors with higher precision are required. A high-Tc SQUID beam current monitor was therefore innovated by one of the authors [13], and long-term testing is scheduled for next fiscal year.

Plastic scintillators (PS) are also introduced in the beam lines. Six pairs of appropriately spaced plastic scintillators are useful to measure ion time of flight (TOF). The beam energy as determined by the TOF monitors has resolution of 0.1%. PSs installed just before the cyclotrons are mainly used to investigate beam phase width. These TOF and plastic scintillation monitors played essential roles in the beam commissioning of RIBF and RILAC2. In our case, intensity-attenuated beams of 10^6pps or so are directly measured using plastic scintillators with a data acquisition system newly developed on LabVIEW architecture [14]. Due to limitations on maximum beam intensity allowed for PSs, it is currently impossible to quantify the space charge and beam loading effects on longitudinal beam emittance of high-power beams. Overcoming this limitation within a reasonable cost remains a topic for further study.

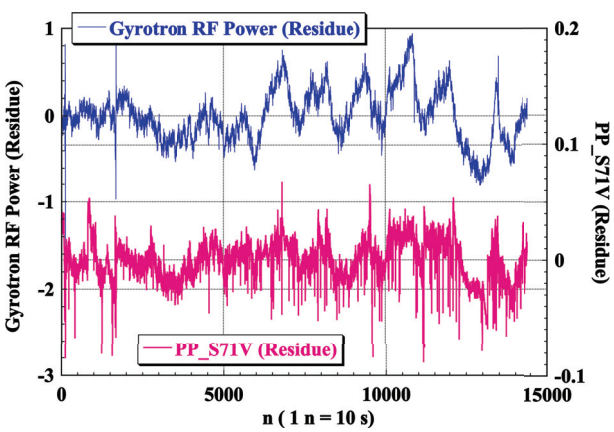

Figure 8: Results of a correlation study between PP signals and RF power for a 28 GHz ECR ion source.

Phase pickup (PP) electrodes are also installed in the beam lines. Signals induced on PPs are pre-amplified (20 dB ~ 40 dB) and analyzed by digital oscilloscopes or lock-in amplifiers similarly as the phase probes of the cyclotrons. PPs are used to determine correct phases of the four rebunchers installed in the beam lines. They are also used for stability analysis of the whole RIBF accelerator complex. Time-varying PP signals are analyzed in correlation with various time series data relevant to accelerator stability, such as magnetic fields, RF fields, power supply currents, cooling water and air temperatures, and commercial electricity. These are continuously monitored and displayed in real time by an integrated system developed by one of the authors [12]. Figure 8 shows an example correlation analysis in which insufficient stability of a gyrotron power supply used in the 28 GHz superconducting ECR ion source [15] drove beam intensity fluctuations. These fluctuations were detected as voltage fluctuations in the PP signals measured at the beam line's S71 position (just before RRC injection). The power supply causing the problem has been replaced.

SUMMARY

RIBF has been steadily upgrading beam intensity for all atomic mass regions by using conventional beam monitors, mainly destructive ones. The maximum beam power obtained is 6.9 kW, near the limits of destructive beam monitors. Development of nondestructive monitors is an important issue for future RIBF upgrade.

REFERENCES

[1] Y. Yano; Nucl. Instr. Meth. B261 p. 1009 (2007), doi:10.101b/ j.nimb.2007.04.174.
[2] N. Fukunishi et al., PAC09, Vancouver, May 2009, MO3GRI01.
[3] M. Odera et al.; Nucl. Instrum. Methods A227, p. 187 (1984).
[4] O. Kamigaito et al., Proc. of PASJ2-LAM30, WP78, (2006). K. Yamada et al.; Proceedings of IPAC'10, Kyoto, Japan, MOPD046 (2010).
[5] A. Goto et al., Proc. 12th Int. Cyclo. Conf. p.51 and p. 439 (1989).
[6] Y. Yano; Proc. 13th Int. Cyclo. Conf. p. 102 (1992).
[7] T. Mitsumoto et al.; Proc. 17th Int. Conf. on Cyclotrons and Their Applications, p. 384 (2004).
[8] J. Ohnishi et al., Proc. 17th Int. Conf. on Cyclotrons and Their Applications, p. 197 (2004).
[9] H. Okuno et al., Proc. 17th Int. Conf. on Cyclotrons and Their Applications, p. 373 (2004). H. Okuno et al., IEEE Trans. Appl. Supercond., **18** (2008) 226.
[10] H. Ryuto et al., Proc. 17th Int. Conf. on Cyclotrons and Their Applications, p. 307 (2004).
[11] http://thinksrs.com/products/SR844.htm, Stanford Research Systems.
[12] R. Koyama; Proc. of EPAC08, Genoa, Italy, TUPC052 (2008).
[13] T. Watanabe et al., Proc. of BIW10, Santa Fe, New Mexico, US, WEIANB02 (2010). T. Watanabe et al., Proc. of IPAC'11, San Sebastian, Spain, PP.1260-1262 (2011).
[14] T. Watanabe et al., RIKEN Accel. Prog. Rep. **43**, 135 (2010).
[15] T. Nakagawa et al., Rev. Sci. Instrum. **79** 02A327 (2008). T. Nakagawa et al., Rev. Sci. Instrum. **81** 02A320 (2010).

ISBN 978-3-95450-119-9